Journal of Fluorine Chemistry 130 (2009) 151–157

Contents lists available at ScienceDirect

Journal of Fluorine Chemistry

journal homepage: www.elsevier.com/locate/fluor

# [2 + 2] Photodimerization and photopolymerization of diphenylhexatriene crystals utilizing perfluorophenyl–phenyl stacking interactions

Yoriko Sonoda [a,*], Midori Goto [b], Seiji Tsuzuki [c], Haruhisa Akiyama [a], Nobuyuki Tamaoki [a]

[a] Nanotechnology Research Institute, National Institute of Advanced Industrial Science and Technology (AIST), Higashi 1-1-1, Tsukuba, Ibaraki 305-8565, Japan
[b] Technical Center, AIST, Higashi 1-1-1, Tsukuba, Ibaraki 305-8565, Japan
[c] Research Institute of Computational Sciences, AIST, Umezono 1-1, Tsukuba, Ibaraki 305-8568, Japan

ARTICLE INFO

*Article history:*
Received 11 August 2008
Received in revised form 17 September 2008
Accepted 17 September 2008
Available online 30 September 2008

*Keywords:*
Perfluorophenyl–phenyl stacking interaction
[2 + 2] Photocycloaddition
Conjugated polyene
Crystal
Amorphous
Powder X-ray diffraction
Polarizing optical microscopy
Non-topochemical
Disorder

ABSTRACT

Irradiation of the crystal of 1-perfluorophenyl-6-phenyl-1,3,5-hexatriene (**1**), the 1:1 cocrystal of 1,6-diphenyl-1,3,5-hexatriene (**2**) and 1,6-bis(perfluorophenyl)-1,3,5-hexatriene (**3**) (**2/3**), and crystal **3** gave a mixture of dimer, trimer and higher oligomers that was soluble in common organic solvents. The highest molecular weight was 5000–8000 (the degree of polymerization = 15–20). The order of reactivity was **1** > **2/3** ≫ **3**. The reaction of **1** was relatively efficient compared to typical organic crystals. The conversion reached 100% after 3 h irradiation. In each case, the regio- and stereoselectivity in the photodimerization was high, whereas in the formation of trimer and higher oligomers, the selectivity was much lower. The main dimer was spectroscopically identified to be the face-to-face dimer formed by the [2 + 2] cycloaddition at the 1,2-position of the triene double bonds. The photoproducts from **1** and **2/3** were amorphous, as evidenced by powder X-ray diffraction and polarizing optical microscopy. This is probably due to the nonplanar and bulky structures of the cyclobutane products. The photodimerization and polymerization are considered to be non-topochemical reactions.



## 1. Introduction

[2 + 2] Cycloaddition is one of the most common photoreactions of olefinic compounds in the solid state [1–3]. The reaction is very useful in synthetic organic chemistry for constructing cyclobutane backbones that are difficult to obtain by other methods [4,5]. As for the crystalline-state [2 + 2] photopolymerization, the reactions of aromatic diolefins such as distyrylpyrazines [6] and phenylene diacrylates [7] are well known. In most cases, the reactions occurred topochemically to afford highly crystalline polymers with cyclobutane rings in the main chain.

α,ω-Diarylpolyenes, having potentially reactive conjugated double bonds, are expected to undergo [2 + 2] photoaddition to give polymeric cyclobutane compounds of a new type with a linear or a zigzag chain structure. As for 1,4-diaryl-1,3-butadienes, there have been several examples reported up to now [8–12]. However, these mainly describe the formation of dimers and occasionally trimers [12], and the polymerization to give higher molecular weight (MW) products has not been reported yet. For 1,6-diaryl(Ar)-1,3,5-hexatrienes, we have previously reported that the unsubstituted parent compound **2** (Fig. 1) was photostable, whereas its ring-substituted (Ar = 4-cyanophenyl and 4-formylphenyl) derivatives underwent photocycloaddition to yield oligomeric mixtures as pale-yellow powderic materials [13]. Although the crystal structures of the two photoreactive derivatives are unknown at present, a face-to-face molecular arrangement [14] and the shortest distance of 3.4–3.6 Å between the triene chains of the neighboring molecules [15] have been suggested for the formyl derivative. Also in these cases, however, the reactions were not very efficient and the MW of the products were relatively low (up to tetramer), as is often seen in organic solids. The 2,4-dichloro substitution, known as very effective to steer solid-state [2 + 2] photoaddition of aromatic molecules, was unsuccessful [16].

Fluorination of aromatic rings often affords single crystals of quality suitable for X-ray analysis. In particular, the noncovalent interactions between $-C_6F_5$ and $-C_6H_5$ groups are known to be strongly attractive, and have been widely used in crystal engineering as a supramolecular synthon to steer face-to-face stacking geometry of aromatic molecules [17–22]. The interactions

* Corresponding author. Tel.: +81 29 861 6390; fax: +81 29 861 4673.
*E-mail address:* y.sonoda@aist.go.jp (Y. Sonoda).

0022-1139/$ – see front matter © 2008 Elsevier B.V. All rights reserved.
doi:10.1016/j.jfluchem.2008.09.010

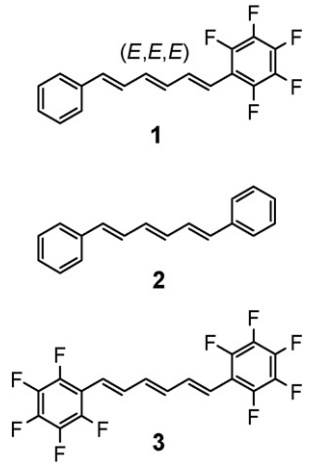


**Fig. 1.** Chemical structures of **1–3**.

were utilized to prealign molecules for the crystalline-state [2 + 2] photocycloaddition of distyrylbenzenes [23] and also for the photopolymerization of diacetylenes [24,25].

We have recently reported the crystal structures and emission properties of a series of ring-fluorinated diphenylhexatrienes [26]. In the course of our study, we found that crystal **1**, 1:1 cocrystal **2/3**, and crystal **3** (Fig. 1) were photopolymerizable. The molecules in these crystals were all arranged in a π-stacking fashion as shown in Fig. 2. In particular, the molecular arrangements in **1** and **2/3** closely resembled each other due to $C_6F_5\cdots C_6H_5$ interactions. In this study, the crystalline-state photodimerization and polymerization of **1**, **2/3** and **3** were investigated in detail.

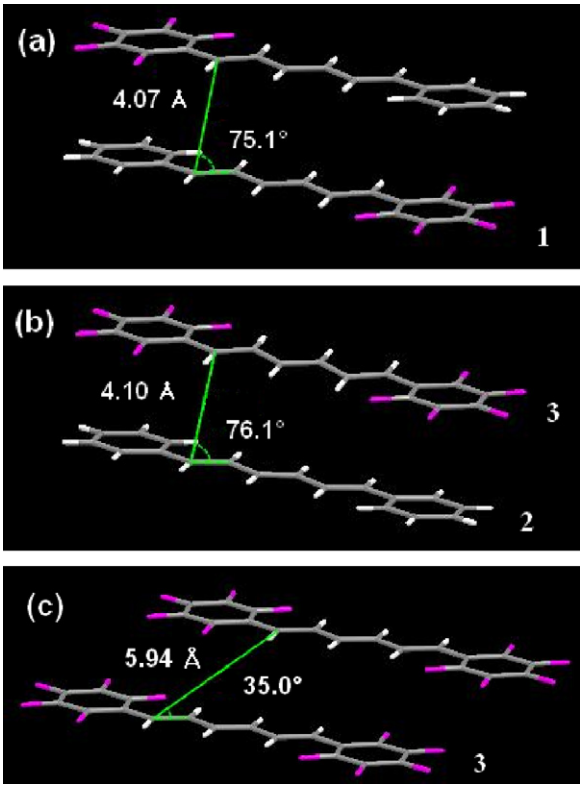


**Fig. 2.** Stacking arrangements of molecules in the crystals of (a) **1**, (b) **2/3** and (c) **3**. Colors: carbon, gray; fluorine, pink; hydrogen, white. (For interpretation of the references to color in this figure legend, the reader is referred to the web version of the article.)

## 2. Results and discussion

### 2.1. Photodimerization and photopolymerization in the crystalline state

#### 2.1.1. Reaction efficiency and degree of polymerization

Irradiation of the yellow crystal of **1** with $\lambda > 340$ nm light in air at room temperature gave somewhat sticky, pale-yellow and transparent solid. Whereas, the yellow crystals of **2/3** and **3** became pale-yellow powder upon irradiation. The photoproducts from **1**, **2/3** and **3** were all soluble in common organic solvents such as dichloromethane and acetonitrile.

GPC analysis showed that the photoproduct in each case was a mixture of dimer, trimer, and higher oligomers with the highest MW of 5000–8000 (the degree of polymerization (DPn) = 15–20). Table 1 summarizes the irradiation time, the conversion, and the content of each GPC fraction for the reactions of **1**, **2/3** and **3**. The order of reactivity was **1** > **2/3** ≫ **3**. Although the molecular arrangements in crystals **1** and **2/3** closely resembled each other, the photoreaction of **1** proceeded considerably faster than that of **2/3**. HPLC analyses showed that *E–Z* photoisomerization of the triene double bond did not take place in these crystals.

The reaction of **1** was relatively efficient compared to typical organic crystals. The conversion reached 100% only after 3 h irradiation. The reaction efficiency and the highest MW were significantly enhanced when compared to those for the cyano- and the formyl-substituted diphenylhexatrienes which we reported previously [13]. This is clearly due to the effective $C_6F_5\cdots C_6H_5$ stacking interactions leading to the molecular arrangements in crystals suitable for the photoreactions. Fig. 3 shows the GPC fraction content as a function of the irradiation time for **1**. As seen, MW did not increase any more after monomer **1** was exhausted. This suggests that, at least using $\lambda > 340$ nm light, the photoexcited species in the reaction is only the monomer.

In the case of **2/3**, the reaction seemed to stop after 3 h, leaving a large amount of monomers **2** and **3** unreacted. The monomers were left in the crystal in the exact molar ratio of **2** and **3** = 1:1, suggesting that the photoproducts were formed by the reaction of equimolar amounts of **2** and **3**. Considering the crystal structure of **2/3**, in which molecules **2** and **3** are stacked alternatively (Fig. 2), the result is quite reasonable. Crystal **3** was also photoreactive, although the efficiency was much lower than those of **1** and **2/3**.

**Table 1**
Conversion and GPC fraction content vs. irradiation time.

| | | | content (w/w %) | | | | | |
|---|---|---|---|---|---|---|---|---|
| | | | GPC fraction | | | | | |
| crystal | irradiation time (h) | conversion (%) | #1 DPn[a] = 1 | #2 2 | #3 3 | #4 4 | #5 6-8 | #6 15-20 |
| **1** | 1 | 56 | 44 | 25 | 12 | 5 | 9 | 5 |
| | 3 | 100 | 0 | 34 | 23 | 15 | 18 | 10 |
| **2/3** | 1 | 28 | 72[b] | 14 | 11 | 3 | 0 | 0 |
| | 3 | 56 | 44[b] | 19 | 12 | 7 | 9 | 9 |
| | 6 | 52 | 48[b] | 17 | 14 | 6 | 9 | 6 |
| | 12 | 65 | 35[b] | 17 | 16 | 10 | 10 | 12 |
| **3** | 6 | 26 | 74 | 9 | 8 | 7 | | 2 |

[a] Polystyrene standard.
[b] Molar ratio of **2**:**3** = 1:1.

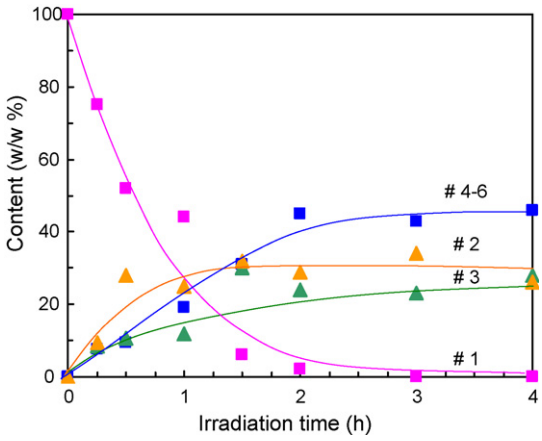


**Fig. 3.** Changes in the content of each GPC fraction during the photoreaction of **1**.

We also examined the thermal reactivity of **1**, **2/3** and **3** for comparison. The crystals were heated in the dark at 110 °C for 6 h in air. In each case, no sizable amount of compound other than the starting material was detected by HPLC.

*2.1.2. Chemical structures of photoproducts*

For **1**, **2/3** and **3**, the HPLC analysis of the GPC fraction #2 (Table 1) showed that only one kind of compound was predominantly formed. They were isolated as main dimers and spectroscopically characterized.

The molecules in crystal **1** are arranged in an anti-parallel fashion (Fig. 2). Therefore, as the main dimer, the face-to-face and syn-head-to-tail dimer formed by the [2 + 2] cycloaddition(s) at the triene double bonds would be the most probable. The multiplet peaks at around $\delta$ 4.2, 4.1, 4.0 and 3.9 ppm in the $^1$H NMR spectrum indicate the presence of four different kinds of cyclobutane ring protons. The doublet to multiplet peaks in the region of 6–7 ppm are clearly assigned to the protons of conjugated dienes with *E*,*E* configuration. In the $^{19}$F NMR spectrum, the peaks due to $C_6F_5$ were clearly observed. Related vicinal $C_6F_5\cdots C_6H_5$ interaction was reported in a recent paper [27]. The MS peak at 270 ($C_6F_5$–CH–CH–$C_6H_5$ fragment) strongly suggests the cycloaddition at the 1,2-position of the trienes. The IR peak at 998 cm$^{-1}$ is attributed to the C–H out-of-plane deformation of *E*,*E* conjugated dienes. The absorption at 282 nm in the UV–vis spectrum shows the main chromophore to be Ar–CH = CH–CH = CH– (Ar = $C_6F_5$ or $C_6H_5$) group. Based on these data, the main photodimer from **1** was identified to be **4**, whose chemical structure is shown in Fig. 4. Similarly, the main dimers from **2/3** and **3** were spectroscopically identified as cyclobutane compounds **5** and **6**, respectively. Unfortunately, however, **4–6** did not seem to be very stable. At least in solution, thermal isomerization was suggested by GPC and HPLC analyses.

In addition to the main dimer, a few kinds of compounds were detected in the GPC fraction #2 by HPLC in all cases. The HPLC data of these minor dimers were similar to those of the thermal isomerization products from the main dimer. Considering the possible isomerization of the main dimer during the GPC purification process of fraction #2 followed by the HPLC analysis in solution, it is very likely that the minor dimers were formed as the secondary products from the main dimer. This agrees with the fact that the product ratio of the minor dimers to the main dimer was somewhat varied in each experiment.

Irradiation of **1** also gave a considerably large amount of trimers (Table 1). The GPC fraction #3 was shown by HPLC analysis to be a complex mixture of several kinds of trimers. Clearly, the regio- and stereoselectivity in the trimer formation was lower than in the dimer formation.

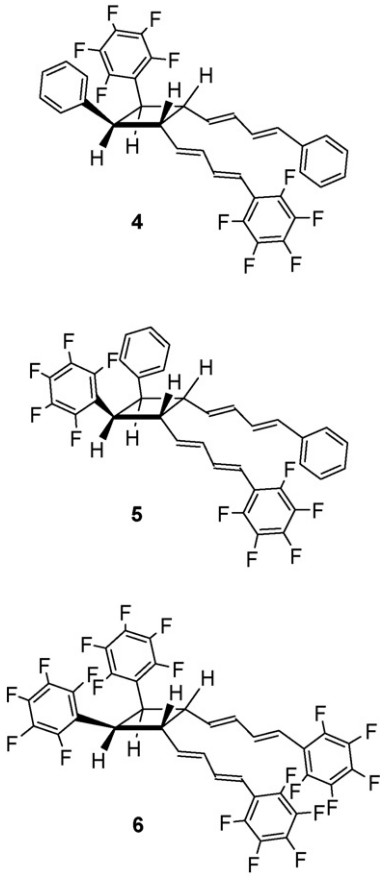


**Fig. 4.** Chemical structures of **4–6**.

Each trimer shows a similar UV–vis spectrum with the main absorption band at 255 nm with the shoulder at 290 nm, suggesting the main chromophores to be Ar– and Ar–CH = CH–CH = CH– (Ar = $C_6F_5$ or $C_6H_5$) groups. The complete spectroscopic identification of each trimer was impossible due to a very limited amount of the product. However, for the mixture of trimers, the presence of the cyclobutane ring and the diene moiety is shown by the broad and multiple NMR peaks in the regions of 3.0–4.2 and 5.6–6.5 ppm, respectively. A small peak was observed at 5.5 ppm, which can be attributed to the olefinic protons of isolated monoenes. The IR spectrum of the trimer mixture was similar to that of **4**. One of the plausible structures of the trimer, a zigzag chain structure, is shown in Fig. 5.

The spectroscopic data of the trimers of **2/3** and **3** suggest similar structures.

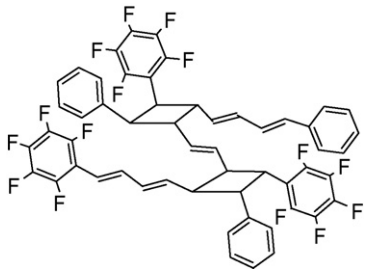

**Fig. 5.** A possible structure of trimer from **1**.

A considerable amount of a mixture of higher oligomers was also obtained from **1** and **2/3**, but they could not be isolated.

### 2.2. Photoreactions in solution

To compare with the photodimerization and polymerization in the crystalline state, the photoreactions of **1**, the mixture of **2** and **3**, and **3** were investigated in toluene solution. The results are summarized in Table 2.

The reaction of **1** in solution was inefficient relative to that in the solid state. The GPC fraction #2 was shown by HPLC analysis to be a mixture of at least nine kinds of dimers. The selectivity in the dimer formation was much lower in solution than in the solid state. The solution reaction of **3** similarly occurred inefficiently to give a complex mixture of low MW oligomers. In contrast, irradiation of an equimolar mixture of **2** and **3** in toluene resulted in the rapid consumption of the monomers to give a very complex mixture of dimer, trimer, and higher oligomers. In addition, a small amount of the oxygenated product, the endo-peroxide of **2**, was formed. For the fluorine-containing **1** and **3**, the photo-oxygenation was inefficient.

The low efficiency for the reactions of **1** and **3** can be attributed to the disordered orientation of molecules in solution, although the reason for the unexpectedly high reactivity observed for the mixed solution of **2** and **3** is unclear at present. The relatively low solubility of the molecules in this solvent would be another reason. The disorderness of molecular orientation should also result in the very low selectivity in the solution reactions. Additionally, the presence of *Z–E* geometrical isomers around the triene double bonds, as evidenced by UV–vis spectroscopy, and the s-*cis*-s-*trans* conformational isomers around the triene single bonds in solution [28], will lead to the formation of many kinds of products.

### 2.3. Powder X-ray diffraction (XRD) patterns

Fig. 6 shows the powder XRD patterns before and after the irradiation of crystal **1**. On irradiation, the intensities of the sharp peaks due to crystalline monomers decreased, and the broad peak centered at $2\theta = 22.04^\circ$ ($d = 4.03$ Å) was rapidly growing up. After 2 h, the original peaks of monomers almost completely disappeared and only the broad peak was observed. This indicates that the photoproducts from **1** are amorphous.

In the case of **2/3**, the sharp peaks of monomers decreased in intensity but remained in the pattern even after 3 h, which agreed with the conversion data in Table 1. However, as in the case of **1**, a new broad peak appeared at $2\theta = 21.48^\circ$ ($d = 4.14$ Å) upon irradiation, and overlapped the original peaks of monomers. Thus, the photoproducts from **2/3** are also found to be amorphous.

For **3**, such a broad peak characteristic of amorphous solids was not clearly observed even after 6 h, although the baseline level of the pattern slightly increased with the progress of the reaction.

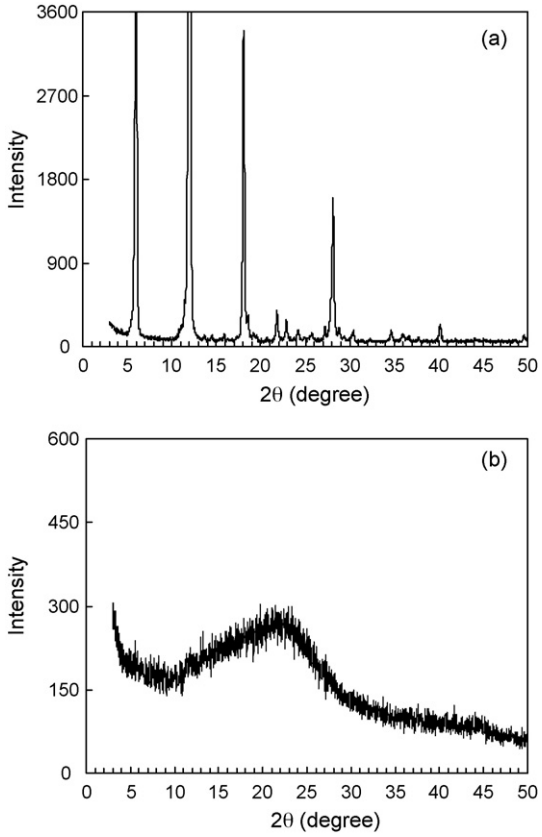


**Fig. 6.** Powder XRD patterns of crystal **1** (a) before and (b) after 2 h irradiation.

**Table 2**
GPC fraction content after 6 h irradiation in toluene.

| compound | content (w/w %) | | |
|---|---|---|---|
| | GPC fraction | | |
| | #1 | #2 | #3 |
| | DPn[c] = 1 | 2 | 3≦ |
| **1**[a] | 93 | 7 | trace |
| **2** + **3**[b] | **2**: 2<br>**3**: 21 | 55 | 22 |
| **3**[a] | 81 | 12 | 7 |

[a] [**1**] = [**3**] = $4.4 \times 10^{-3}$ M.
[b] [**2**] = [**3**] = $2.2 \times 10^{-3}$ M.
[c] Polystyrene standard.

### 2.4. Polarizing optical micrographs

Fig. 7 shows the changes in the polarizing optical micrographs of crystal **1** during irradiation. Crystal **1** was irradiated to transform rapidly to isotropic materials from the peripheral of the crystal. After 30 min, the reaction was completed and the crystal became almost completely transparent. Thus, in agreement with the observations in the XRD patterns, the photoproducts are shown to be amorphous. As clearly seen, the photoproducts were amorphous even at the initial stages of the reaction, while the unreacted monomers kept crystalline even at the very later stages of the reaction. The photoreaction appeared to take place at the interface of the crystalline and the amorphous phases. A similar two-phase reaction has been reported for the radiation-induced solid-state polymerization of acrylamide [29].

The changes in the micrographs of crystal **2/3** were similar. Unlike **1**, however, stripe-like microstructures formed very rapidly just after the irradiation started. On further irradiation, the structures disappeared gradually and then a transparent part was slowly growing up from the edge of the crystal. Although the mechanism for the formation of microstructure is unclear at present, this may be responsible for the reduced reaction rate of **2/3** relative to that of **1**.

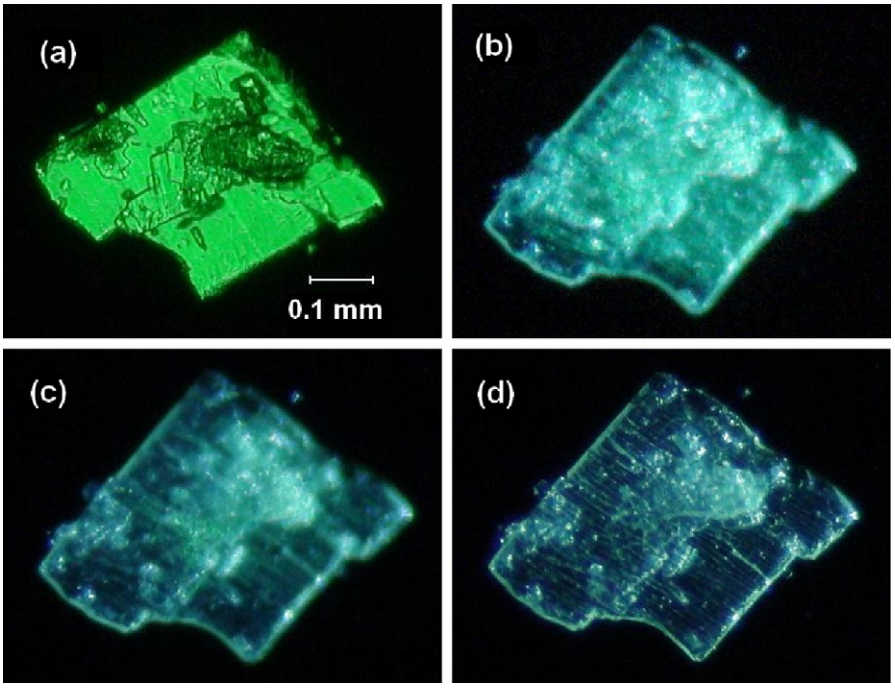


**Fig. 7.** Polarizing optical micrographs of crystal **1** (a) before and after irradiation for (b) 14 min, (c) 20 min, and (d) 30 min.

### *2.5. Molecular movements in crystals during photodimerization and photopolymerization*

#### *2.5.1. Reactions of 1 and 2/3*

Before irradiation, the molecules in crystal **1** are regularly arranged in an anti-parallel fashion due to the $C_6F_5\cdots C_6H_5$ intermolecular interactions (Fig. 2). The high regio- and stereoselectivity in the photodimerization of **1** clearly results from the prealignment of molecules in the original crystal.

Fig. 8 shows the optimized structure of **4** by molecular orbital calculation. As seen, the dimer is predicted to be completely nonplanar and very bulky. It is therefore, very probable that the formation of **4** will be accompanied by the very large changes in molecular shape and volume from those of the reacting two molecules before irradiation, and should consequently break the ordered arrangement of the neighboring molecules in the crystal. In the resulting disordered crystal structure should occur the subsequent formation of trimers and higher oligomers randomly. This accounts for the low selectivity in the trimer formation relative to that in the dimer formation. The photodimerization and polymerization of **1** are thus, considered to be non-topochemical reactions.

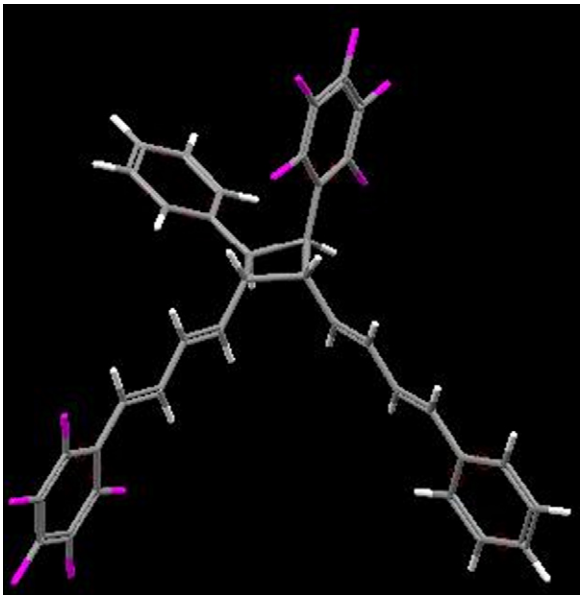

**Fig. 8.** Optimized structure of **4**.

The high reaction efficiency of **1** compared to typical organic crystals is probably because the molecular movements are much easier in amorphous solids than in ordinary rigid crystals. This is consistent with the facts that the photoexcited species was only the monomer, and that the reaction seemed to take place at the interface of the crystalline part of monomers and the amorphous part of the photoproducts. Also, it is probable that the transparency of the amorphous products made the irradiation light reach inside of the crystal, leading to the efficient photoreaction. The efficient photoreaction due to the transparency of the products was similarly observed for the crystalline-state *Z*–*E* photoisomerization of (*Z*,*E*,*Z*)-1,6-diphenyl-1,3,5-hexatrienes [30]. Considering that molecules with nonplanar and bulky structures tend to be amorphous in the solid state [31,32], the formation of the amorphous states of products in the present case should mainly be attributed to the molecular shape of **4** itself (and probably those of the trimer and higher oligomers themselves).

Besides the formation of the stripe-like structures observed in the micrographs in the earlier stages of the reaction, the main features of the photoreaction of **2**/**3** are fundamentally the same as those of **1**, and can be understood similarly.

With a few exceptions [33], the crystalline-state [2 + 2] photopolymerization of distyrylpyrazines and phenylene diacrylates took place topochemically to afford highly crystalline polymers [6]. Ring-fluorinated distyrylbenzene crystals have also been reported to be photopolymerizable [23]. In this case, the product was a powder that was virtually insoluble, or a polymeric product that was partially soluble in organic solvents. In contrast,

the photodimerization and photopolymerization of **1** and **2/3** occurred non-topochemically to give highly soluble, amorphous products. Our present results suggest that cyclobutane compounds, when possessing long and bulky substituents, may be useful as amorphous molecular materials.

*2.5.2. Reaction of 3*

The offset for the stacking molecules in crystal **3** is larger than those in **1** and **2/3** [26], as a result of weak $C_6F_5\cdots C_6F_5$ intermolecular interactions relative to $C_6F_5\cdots C_6H_5$ interactions [34] (Fig. 2). For the reacting two molecules of **3** in the stack, the distance between the triene carbons at the 1-position is 5.94 Å, which is considerably larger than the (normal) upper limit of 4.2 Å for the [2 + 2] photocycloaddition ('4.2 Å-rule') [1]. [2 + 2] Cycloadditions are in general considered to proceed via excimers. Indeed, crystal **3** exhibited solid-state excimer fluorescence, indicating the presence of some intermolecular interactions in the excited state [26]. Although we cannot, of course, entirely exclude the possibility that the reaction of **3** takes place from some structural defects in the crystal, it may be possible that molecule **3** is irradiated to move in the crystal, making the intermolecular cycloaddition possible. Also for the several exceptions to the 4.2 Å-rule reported up to now, the molecular movements in the excited states (or the dynamic preformation of excimers in the crystal lattice) are suggested [1,10,35–38].

## 3. Conclusions

The $C_6F_5\cdots C_6H_5$ stacking interactions were effectively utilized to control the photoreactions of diphenylhexatrienes in the crystalline state. Irradiation of the crystals of **1**, **2/3**, and **3** induced [2 + 2] photodimerization and photopolymerization. The order of reactivity was **1** > **2/3** ≫ **3**. The reaction of **1** was relatively efficient compared to typical organic crystals. In each case, the regio- and stereoselectivity in the photodimerization was high, whereas in the formation of trimer and higher oligomers, the selectivity was much lower. The photoproducts from **1** and **2/3** were amorphous, as evidenced by powder XRD and polarizing optical microscopy. This is probably due to the nonplanar and bulky structures of the cyclobutane products. The high reaction efficiency of **1** can be attributed to much easier molecular movements in amorphous solids than in ordinary rigid crystals. The high selectivity in the dimerization clearly results from the anti-parallel prealignment of molecules in the original crystal. Whereas, the formation of trimers and higher oligomers occurs randomly in the disordered crystal structure produced by the dimer formation, which explains the low selectivity in the trimer formation relative to that in the dimer formation.

## 4. Experimental

### 4.1. General experimental procedures

HR- and LR-MS were obtained using a Hitachi M-80B instrument. FAB-MS were obtained with a JEOL MS-600H spectrometer. IR spectra were measured on a Mattson Infinity Gold FT-IR spectrometer. $^1$H NMR spectra were recorded on a Varian Gemini-300 BB spectrometer (300 MHz) with tetramethylsilane as internal reference. $^{19}$F NMR spectra were recorded on a JEOL ECA-300 spectrometer (283 MHz), and were referenced to hexafluorobenzene at 0.0 ppm. Measurements of MW and purification of photoproducts were carried out using a Japan Analytical Industry LC-908 recyclable GPC with chloroform eluent. Photoproducts were analyzed by a TOSOH CCPD/SD-8013/SC-8020 reverse-phase HPLC monitored by a Photal MCPD-3600 multichannel photodetector with acetonitrile eluent. A Merck LiChroCART250-4 column filled with Lichrosorb RP-18 (5 μm) was used.

### 4.2. Characterization

The preparation procedures of crystals **1**, **2/3**, **3** have been described previously [26].

*Dimer* **4**. HR-MS ($[M]^+/2$) calculated for $C_{18}H_{11}F_5$ 322.0779, found 322.0761; LR-MS 322 ($C_{18}H_{11}F_5$, 100%), 270 ($C_6F_5$–CH–CH–$C_6H_5$, 13%), 129 ($C_6H_5$–CH = CH–CH = CH–, 8%), 103 ($C_6H_5$–CH = CH–, 9%), 77 ($C_6H_5$–, 16%); FAB-MS $[M^+]$ = 644; IR (KBr) $\nu$ 3029, 2926, 2851, 1727, 1654, 1602, 1522, 1498, 1128, 998, 963, 740 and 701 cm$^{-1}$; $^1$H NMR ($CDCl_3$) $\delta$ 7.02–7.42 (12H, m), 6.81 (1H, dd, $J$ = 15.7 and 10.3 Hz), 6.52 (1H, d, $J$ = 15.7 Hz), 6.39 (1H, d, $J$ = 16.1 Hz), 6.26–6.44 (2H, m), 6.05 (1H, dd, $J$ = 15.1 and 8.1 Hz), 4.20–4.26 (1H, m), 4.05–4.14 (1H, m), 3.98–4.03 (1H, m), 3.84–3.91 (1H, m); $^{19}$F NMR ($CDCl_3$) $\delta$ 18.7–20.4 (4F, m), 6.0 (2F, br), −1.0 (4F, br); UV–vis ($CH_3CN$) $\lambda_{max}$ 282 nm.

*Dimer* **5**. HR-MS ($[M]^+$-**3**) calculated for $C_{18}H_{16}$ 232.1251, found 232.1128; ($[M]^+$-**2**) calculated for $C_{18}H_6F_{10}$ 412.0309, found 412.0318; LR-MS 412 ($C_{18}H_6F_{10}$, 57%), 270 ($C_6F_5$–CH–CH–$C_6H_5$, 36%), 232 ($C_{18}H_{16}$, 100%), 219 ($C_6F_5$–CH = CH–CH = CH–, 7%), 167 ($C_6F_5$–, 23%), 129 ($C_6H_5$–CH = CH–CH = CH–, 27%), 103 ($C_6H_5$–CH = CH–, 34%), 77 ($C_6H_5$–, 74%); FAB-MS: $[M^+ + 1]$ = 645, $[M^+ - 1]$ = 643; IR (KBr) $\nu$ 1711, 1653, 1600, 1523, 1498, 1130, 997, 963 and 700 cm$^{-1}$; $^1$H NMR ($CDCl_3$) $\delta$ 7.05–7.43 (12H, m), 6.83 (1H, dd, $J$ = 15.6 and 10.3 Hz), 6.51 (1H, d, $J$ = 15.8 Hz), 6.40 (1H, d, $J$ = 15.9 Hz), 6.19–6.35 (2H, m), 6.12 (1H, dd, $J$ = 15.1 and 8.1 Hz), 4.22–4.28 (1H, m), 4.07–4.15 (1H, m), 3.96–4.02 (1H, m), 3.82–3.90 (1H, m); $^{19}$F NMR ($CDCl_3$) $\delta$ 18.8–20.7 (4F, m), 5.7 (2F, br), −1.0 (4F, br); UV–vis ($CH_3CN$) $\lambda_{max}$ 282 nm.

*Dimer* **6**. HR-MS ($[M]^+/2$) calculated for $C_{18}H_6F_{10}$ 412.0309, found 412.0271; LR-MS 412 ($C_{18}H_6F_{10}$, 100%), 360 ($C_6F_5$–CH–CH–$C_6F_5$, 10%), 219 ($C_6F_5$–CH = CH–CH = CH–, 66%), 193 ($C_6F_5$–CH = CH–, 52%), 167 ($C_6F_5$–, 21%); FAB-MS: $[M^+]$ = 824; IR (KBr) $\nu$ 1713, 1652, 1522, 1496, 1123, 996 and 962 cm$^{-1}$; $^1$H NMR ($CDCl_3$) $\delta$ 6.92 (2H, dd, $J$ = 16.0 and 10.4 Hz), 6.37 (2H, d, $J$ = 16.1 Hz), 6.21 (2H, dd, $J$ = 14.6 and 10.2 Hz), 5.89 (2H, dd, $J$ = 15.1 and 8.5 Hz), 4.30–4.36 (2H, m), 4.11–4.19 (2H, m); $^{19}$F NMR ($CDCl_3$) $\delta$ 20.5–20.6 (4F, m), 19.0–19.1 (4F, m), 6.7–6.9 (2F, m), 5.6–5.7 (2F, m), 0.1–0.3 (4F, m), (−1.3) – (−1.1) (4F, m); UV–vis ($CH_3CN$) $\lambda_{max}$ 295 nm.

### 4.3. Irradiation experiments

In the irradiation experiments for the GPC and HPLC product analyses and the powder XRD measurements, a high-pressure mercury lamp (500 W, 10.0 mW/cm$^2$) was used as a light source. The light was filtered with glass filters ($\lambda > 340$ nm). For the product analyses, the crystals of **1**, **2/3** and **3** were placed between quartz plates and irradiated. The irradiation was interrupted every 50–60 min by standing in the dark for 10 min to prevent any thermal reaction. The sample crystals were not ground to a powder.

In the irradiation experiments to monitor the reactions by polarizing optical microscopy, a high-pressure mercury lamp (250 W, 18.4 mW/cm$^2$) was used as a light source ($\lambda > 340$ nm). Sample crystals were placed on a glass substrate and irradiated.

### 4.4. Powder XRD measurements

The powder XRD measurements of **1**, **2/3** and **3** were performed at room temperature using a Rigaku Ultima III diffractometer (parallel beam optics) with graphite monochromated Cu Kα radiation (λ = 1.5418 Å). The sample crystals were lightly ground

before measurements, placed on a low background sample holder made of silicon, and irradiated.

### 4.5. Computational method

The Gaussian 03 program [39] was used for the ab initio molecular orbital calculations. The ground-state geometry of **4** was optimized at the HF/6-31G* level.

## Acknowledgments

We thank Dr. M. Sakashita (AIST) for her help in the measurements of powder XRD patterns, and Dr. J. Mizukado (AIST) for the measurements of $^{19}F$ NMR spectra.

## References

[1] V. Ramamurthy, K. Venkatesan, Chem. Rev. 87 (1987) 433–481.
[2] K. Tanaka, F. Toda, Chem. Rev. 100 (2000) 1025–1074.
[3] Y. Sonoda, in: W. Horspool, F. Lenci (Eds.), CRC Handbook of Organic Photochemistry and Photobiology, 2nd ed., CRC Press, Boca Raton, 2004, , Chapter 73.
[4] N. Hoffmann, Chem. Rev. 108 (2008) 1052–1103.
[5] L.R. MacGillivray, G.S. Papaefstathiou, T. Friščić, T.D. Hamilton, D.-K. Bučar, Q. Chu, D.B. Varshney, I.G. Georgiev, Acc. Chem. Res. 41 (2008) 280–291.
[6] M. Hasegawa, Adv. Phys. Org. Chem. 30 (1995) 117–171.
[7] S. Takahashi, H. Miura, H. Kasai, S. Okada, H. Oikawa, H. Nakanishi, J. Am. Chem. Soc. 124 (2002) 10944–10945.
[8] M.D. Cohen, A. Elgavi, B.S. Green, Z. Ludmer, G.M.J. Schmidt, J. Am. Chem. Soc. 94 (1972) 6776–6779.
[9] A. Elgavi, B.S. Green, G.M.J. Schmidt, J. Am. Chem. Soc. 95 (1973) 2058–2059.
[10] A.K. Singh, T.S.R. Krishina, J. Phys. Chem. A 101 (1997) 3066–3069.
[11] J. Liu, N.L. Wendt, K.J. Boarman, Org. Lett. 7 (2005) 1007–1010.
[12] Y. Mori, A. Matsumoto, Chem. Lett. 36 (2007) 510–511.
[13] Y. Sonoda, A. Miyazawa, S. Hayashi, M. Sakuragi, Chem. Lett. 30 (2001) 410–411.
[14] S. Hayashi, Y. Sonoda, Bull. Chem. Soc., Jpn. 77 (2004) 2159–2164.
[15] Y. Sonoda, Y. Kawanishi, T. Ikeda, M. Goto, S. Hayashi, Y. Yoshida, N. Tanigaki, K. Yase, J. Phys. Chem. B 107 (2003) 3376–3383.
[16] Y. Sonoda, Y. Kawanishi, M. Goto, Acta Crystallogr. C59 (2003) o311–o313.
[17] K. Reichenbächer, H.I. Süss, J. Hulliger, Chem. Soc. Rev. 34 (2005) 22–30.
[18] D.G. Naae, Acta Crystallogr. B35 (1979) 2765–2768.
[19] G.P. Bartholomew, X. Bu, G.C. Bazan, Chem. Mater. 12 (2000) 2311–2318.
[20] W.J. Feast, P.W. Lövenich, H. Puschmann, C. Taliani, Chem. Commun. (2001) 505–506.
[21] F. Ponzini, R. Zagha, K. Hardcastle, J.S. Siegel, Angew. Chem. Int. Ed. 39 (2000) 2323–2325.
[22] C.E. Smith, P.S. Smith, R.L. Thomas, E.G. Robins, J.C. Collings, C. Dai, A.J. Scott, S. Borwick, A.S. Batsanov, S.W. Watt, S.J. Clark, C. Viney, J.A.K. Howard, W. Clegg, T.B. Marder, J. Mater. Chem. 14 (2004) 413–420.
[23] G.W. Coates, A.R. Dunn, L.M. Henling, J.W. Ziller, E.B. Lobkovsky, R.H. Grubbs, J. Am. Chem. Soc. 120 (1998) 3641–3649.
[24] G.W. Coates, A.R. Dunn, L.M. Henling, D.A. Dougherty, R.H. Grubbs, Angew. Chem. Int. Ed. 36 (1997) 248–251.
[25] R. Xu, V. Gramlich, H. Frauenrath, J. Am. Chem. Soc. 128 (2006) 5541–5547.
[26] Y. Sonoda, M. Goto, S. Tsuzuki, N. Tamaoki, J. Phys. Chem. A 111 (2007) 13441–13451.
[27] T. Korenaga, K. Kadowaki, T. Sakai, J. Fluorine Chem. 128 (2007) 557–561.
[28] J. Saltiel, D.F. Sears, Y.P. Sun, J.O. Choi, J. Am. Chem. Soc. 114 (1992) 3607–3612.
[29] G. Adler, W. Reams, J. Chem. Phys. 32 (1960) 1698–1700.
[30] Y. Sonoda, Y. Kawanishi, S. Tsuzuki, M. Goto, J. Org. Chem. 70 (2005) 9755–9763.
[31] Y. Shirota, J. Mater. Chem. 15 (2005) 75–93.
[32] M.R. Robinson, S. Wang, A.J. Heeger, G.C. Bazan, Adv. Funct. Mater. 11 (2001) 413–419.
[33] F. Nakanishi, H. Nakanishi, M. Hasegawa, Y. Yamada, J. Polym. Sci.: Polym. Chem. Ed. 13 (1975) 2499–2506.
[34] A. Frontera, D. Quiñonero, A. Costa, P. Ballester, P.M. Deyà, New J. Chem. 31 (2007) 556–560.
[35] H. Nakanishi, M. Hasegawa, T. Mori, Acta Crystallogr. C41 (1985) 70–71.
[36] J.H. Kim, M. Matsuoka, K. Fukunishi, Chem. Lett. 28 (1999) 143–144.
[37] M.M.S. Abdel-Mottaleb, S. De Feyter, A. Gesquière, M. Sieffert, M. Klapper, K. Müllen, F.C. De Schryver, Nano Lett. 1 (2001) 353–359.
[38] L.-P. Xu, C.-J. Yan, L.-J. Wan, S.-G. Jiang, M.-H. Liu, J. Phys. Chem. B 109 (2005) 14773–14778.
[39] M.J. Frisch, G.W. Trucks, H.B. Schlegel, G.E. Scuseria, M.A. Robb, J.R. Cheeseman, J.A. Montgomery Jr., T. Vreven, K.N. Kudin, J.C. Burant, J.M. Millam, S.S. Iyengar, J. Tomasi, V. Barone, B. Mennucci, M. Cossi, G. Scalmani, N. Rega, G.A. Petersson, H. Nakatsuji, M. Hada, M. Ehara, K. Toyota, R. Fukuda, J. Hasegawa, M. Ishida, T. Nakajima, Y. Honda, O. Kitao, H. Nakai, M. Klene, X. Li, J.E. Knox, H.P. Hratchian, J.B. Cross, V. Bakken, C. Adamo, J. Jaramillo, R. Gomperts, R.E. Stratmann, O. Yazyev, A.J. Austin, R. Cammi, C. Pomelli, J.W. Ochterski, P.Y. Ayala, K. Morokuma, G.A. Voth, P. Salvador, J.J. Dannenberg, V.G. Zakrzewski, S. Dapprich, A.D. Daniels, M.C. Strain, O. Farkas, D.K. Malick, A.D. Rabuck, K. Raghavachari, J.B. Foresman, J.V. Ortiz, Q. Cui, A.G. Baboul, S. Clifford, J. Cioslowski, B.B. Stefanov, G. Liu, A. Liashenko, P. Piskorz, I. Komaromi, R.L. Martin, D.J. Fox, T. Keith, M.A. Al-Laham, C.Y. Peng, A. Nanayakkara, M. Challacombe, P.M.W. Gill, B. Johnson, W. Chen, M.W. Wong, C. Gonzalez, J.A. Pople, Gaussian 03 Revision C. 02, Gaussian Inc., Wallingford, CT, 2004.